Reviews in Cardiovascular Medicine

Original Research

Abnormal expression of *TGFBR2*, *EGF*, *LRP10*, and *IQGAP1* is involved in the pathogenesis of coronary artery disease

Yanwei Du[1,2,†], Yanan Hu[2,†], Naiyan Wen[3], Shuang Fu[2], Guorong Zhang[2], Li Li[2], Tiantian Liu[2], Xuejiao Lv[1,*], Wenfeng Zhang[2,*]

[1] *Department of Respiratory and Critical Care Medicine, the 2nd Hospital of Jilin University, 130041 Changchun, Jilin, China*

[2] *Department of Prescriptions, Pathology and Pathophysiology, Changchun University of Chinese Medicine, 130117 Changchun, Jilin, China*

[3] *Department of Nursing, Changchun University of Chinese Medicine, 130117 Changchun, Jilin, China*

*Correspondence: wenfzh@163.com (Wenfeng Zhang); lvxuejiao0311@163.com (Xuejiao Lv)
† These authors contributed equally.

DOI:10.31083/j.rcm2203103

Submitted: 22 February 2021 Revised: 14 April 2021 Accepted: 15 July 2021 Published: 24 September 2021

Coronary artery disease (CAD) is the most common cardiovascular disease worldwide. In this study, we investigated the pathogenesis of CAD. We downloaded the GSE98583 dataset, including 12 CAD samples and 6 normal samples, from the Gene Expression Omnibus (GEO) database and screened differentially expressed genes (DEGs) in CAD versus normal samples. Next, we performed functional enrichment analysis, protein-protein interaction (PPI) network, and functional module analyses to explore potential functions and regulatory functions of identified DEGs. Next, transcription factors (TFs) and microRNAs (miRNAs) targeting DEGs were predicted. In total, 456 DEGs were identified in CAD and normal samples, including 175 upregulated and 281 downregulated genes. These genes were enriched in the intestinal immune network for immunoglobulin A production and the mitogen-activated protein kinase signaling pathway (e.g., *TGFBR2* and *EGF*). The PPI network contained 212 genes, and *HIST1H2BJ*, *HIST1H2AC*, *EGF*, and *EP300* were hub genes with degrees higher than 10. Four significant modules were identified from the PPI network, with genes in the modules mainly enriched in the inflammatory response, protein ubiquitination involved in ubiquitin-dependent protein catabolic processes, protein transport, and mitochondrial translational elongation, respectively. Two TFs (E2F1 and FOXK1) and five miRNAs (*miR-122A*, *miR-516-5P*, *miR-507*, *miR-342*, and *miR-520F*) were predicted to target 112 DEGs. *miR-122A* reportedly targets both *LRP10* and *IQGAP1* in the TF-miRNA target regulatory network. The abnormal expression of *TGFBR2*, *EGF*, *LRP10*, and *IQGAP1* may be implicated in CAD pathogenesis. Our study provides targets and potential regulators for investigating CAD pathogenesis.

Keywords

Coronary artery disease; Transcription factor; microRNAs; MAPK signaling pathway; Pathogenesis

1. Introduction

Coronary artery disease (CAD), also known as ischemic heart disease, is a group of diseases that includes sudden cardiac death, myocardial infarction, and stable and unstable angina [1]. CAD is the most common cardiovascular disease and is usually characterized by chest discomfort or chest pain [2]. For CAD, primary risk factors include a lack of exercise, smoking, excessive alcohol consumption, high blood pressure, obesity, depression, and poor diet [3, 4]. Additionally, genetics is considered a risk factor for developing CAD [5]. In clinical practice, CAD can be diagnosed by employing coronary angiography, electrocardiogram, coronary computed tomographic angiography, and cardiac stress testing [6]. In 2015, 110 million CAD cases were reported, leading to 8.9 million deaths, thus making it the leading cause of disease-related deaths globally [7]. Therefore, elucidating mechanisms that underlie CAD is of considerable importance and significance.

Kalirin (*KALRN*) reportedly inhibits the activities of guanine-exchange factor and inducible nitric oxide synthase, which play important roles in the CAD mechanism via the Rho GTPase signaling pathway [8]. Decreased adiponectin and increased interleukin-6 (*IL-6*) levels promote CAD progression in epicardial adipose tissues [9, 10]. Moreover, levels of neuregulin-4 (*Nrg4*) are found to be inversely related to the development and severity of CAD [11]. Transforming growth factor-β1 (*TGF-β1*) is involved in the pathogenesis of restenosis, including thrombogenesis and inflammation. In patients with CAD, polymorphisms and *TGF-β1* levels are independent risk factors for developing in-stent restenosis after coronary bare-metal stent implantation [12]. *MiR-214* is known to inhibit the expression of vascular endothelial growth factor (*VEGF*), as well as activities of endothelial progenitor cells; therefore, circulating *miR-214* could be employed as a novel biomarker and a diagnostic factor for CAD [13]. *MiR-34a* mediates sirtuin 1 (*SIRT1*) in endothelial progenitor cells, and atorvastatin reportedly improves endothelial function by promoting *SIRT1* expression by suppressing *miR-34a* [14, 15]. Serum levels of *miR-126*, *miR-197*, and *miR-223* are reportedly increased in patients with CAD, and both *miRNA-197* and *miRNA-223* can predict cardiovascular death [16]. According to a report by Bai *et al.* [17], the MEG3-miR-26a-Smad1 regulatory axis can be implicated in regulating the proliferation/apoptosis balance of vascular smooth

muscle cells during atherosclerosis. Although these studies have focused on CAD pathogenesis, key genes and miRNAs associated with CAD remain unclear.

Microarray studies of human diseases, including CAD, are limited owing to a lack of human disease tissues or appropriate disease models. Peripheral blood plays a crucial role in mediating immune responses, metabolism, and intercellular communication, as well as affords convenient sample collection; accordingly, it is an ideal tissue for biomarker detection [18, 19]. Moreover, gene expression in peripheral blood could reflect CAD severity [20, 21]. Additionally, Taurino *et al.* [22] revealed that analyzing gene expression in whole blood is useful for detecting genes that determine cardiovascular phenotypes, including those implicated in the pathogenesis and progression of CAD. In the present study, we utilized the microarray dataset GSE98583, contributed by Kumar and Kashyap *et al.* [23]. In the study by Kumar and Kashyap *et al.* [23], differentially expressed genes (DEGs) of different disease severities were identified, followed by functional enrichment and other analyses to explore candidate genes and pathways contributing to CAD severity. In the present study, we primarily identified DEGs in CAD and control samples, followed by functional enrichment and prediction of transcription factors (TFs) and microRNAs (miRNAs) regulating these DEGs, to elucidate potential genes and their corresponding regulators involved in CAD pathogenesis. This study will provide deeper insights into the pathogenesis of CAD and provide a theoretical basis for developing targeted therapy.

2. Methods

2.1 Ethical approval

In the present study, all datasets were downloaded from public databases, which allowed researchers to download and analyze public datasets for scientific purposes. Therefore, ethical approval was not required.

2.2 Data source

We downloaded and used the microarray dataset GSE98583 from the Gene Expression Omnibus (GEO, http://www.ncbi.nlm.nih.gov/geo/) database, which is based on the GPL571 [HG-U133A_2] Affymetrix Human Genome U133A 2.0 Array. The GSE98583 dataset included 12 whole blood samples from non-diabetic male patients with CAD based on their coronary angiogram results. Of the 12 patients, 6 presented single-vessel disease (stenosis >95% in the left anterior descending artery, Gensini score 20–30), and 6 had triple vessel disease (stenosis >95% in all three major epicardial vessels, Gensini score 50–60). Additionally, six whole blood samples from control subjects with atypical angina and normal coronary angiograms were included.

2.3 Data preprocessing and differential expression analysis

The original CEL files were downloaded and preprocessed using the R package Oligo (version 1.34.0, http://bioconductor.org/help/search/index.html?q=oligo/, Johns Hopkins University, Baltimore, MD, USA.) [24]. Data preprocessing involved data format conversion, filling missing data, background correction, and data standardization. Next, the probes were annotated and combined with platform annotation files. Probes that could not be matched to gene symbols were filtered out. For multiple probes mapped to one gene symbol, the average value of the probes was obtained as the expression value of the corresponding gene symbol. Using the R package Limma (version 3.10.3, http://www.bioconductor.org/packages/release/bioc/html/limma.html, Walter and Eliza Hall Institute of Medical Research, Melbourne, Australia) [25], we analyzed DEGs between CAD and control samples. Genes with a *P*-value of <0.05 were defined as DEGs.

2.4 Enrichment analysis

Based on the Database for Annotation, Visualization and Integrated Discovery (DAVID, version 6.8, https://david.ncifcrf.gov/, Laboratory ofHuman Retrovirology and Immunoinformatic, USA) tool [26], Gene Ontology (GO) terms [27] and Kyoto Encyclopedia of Genes and Genomes (KEGG) pathway [28] enrichment analyses were performed for identified DEGs. The number of genes involved in each term was set at ≥ 2, and a *P*-value < 0.05 was established as the significant threshold.

2.5 PPI network analysis

Combined with the STRING (version 10.0, http://string-db.org/) database [29], PPI pairs were used to predict proteins encoded by identified DEGs. The PPI score was set at 0.7. Next, a PPI network was constructed for DEGs using the Cytoscape software (version 3.2.0, http://www.cytoscape.org, National Institute of General Medical Sciences, USA) [30]. Using the CytoNCA plug-in (version 2.1.6, http://apps.cytoscape.org/apps/cytonca Central South University, Changsha, China) [31] in Cytoscape with parameter set as: without weight, we performed network topology analysis to identify the hub network nodes. Furthermore, significant modules with a score >5 were selected from the PPI network using the MCODE plug-in (version 1.4.2, http://apps.cytoscape.org/apps/MCODE, University of Toronto, Canada) [32] in Cytoscape.

2.6 TF-miRNA target regulatory network analysis

Using the iRegulon plug-in (version 1.3, http://apps.cytoscape.org/apps/iRegulon, Laboratory of Computational Biology, KU Leuven, Belgium) [33] in Cytoscape, we performed a TF-target prediction for the PPI network nodes. The parameters "minimum identity between orthologous genes" and "maximum false discovery rate on motif similarity" were set at 0.05 and 0.001, respectively. Results with a normalized enrichment score (NES) of >4 were selected. Using the WebGestalt GAST (version: updata 2013, http://www.webgestalt.org/option.php, Baylor College of Medicine, Houston, TX, USA) tool [34], we predicted target miRNAs for PPI network nodes by employing the overrepresentation enrichment analysis (ORA) method. The least number of enriched genes was

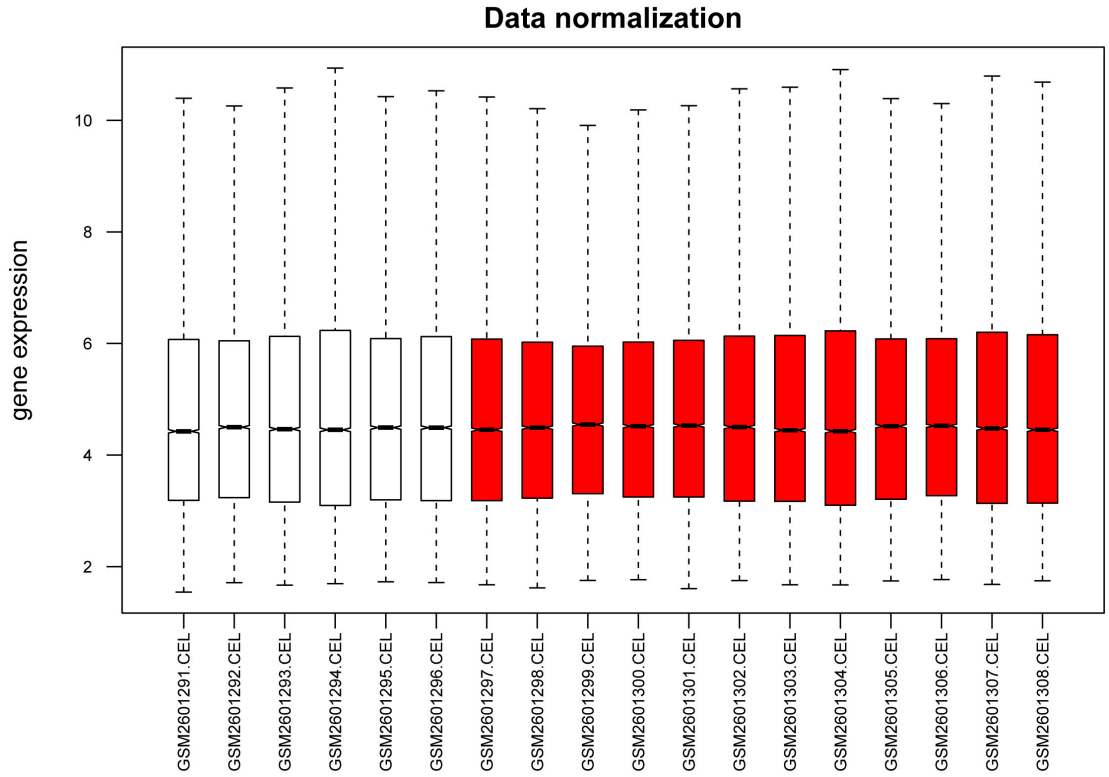

Fig. 1. The box diagram presents the distribution of expression values after data normalization. Red and white represent disease samples and control samples, respectively.

set at two, and the top five results are presented. Finally, the results of TF-target prediction and miRNA-target prediction were merged to build the TF-miRNA target regulatory network using Cytoscape [30].

2.7 Validation using the Comparative Toxicogenomics Database

The etiology of several chronic diseases is based on interactions between environmental chemicals and genes regulating physiological processes [35]. The Comparative Toxicogenomics Database (CTD, http://ctdbase.org/, NC State University, Raleigh, NC, USA) is a publicly available database for identifying chemical-gene-disease networks [36]. We conducted a CTD search to identify genes and pathways associated with CAD. Next, we performed a Venn analysis to identify overlapping genes and pathways between the CTD database and the microarray dataset GSE98583.

3. Results

3.1 Differential expression analysis

The distribution of expression values after data normalization is shown in Fig. 1. The medians were at the same level, indicating that data preprocessing results were good. According to the screening threshold, a total of 456 DEGs (175 upregulated and 281 downregulated genes) were identified. The clustering heatmap indicated that DEGs could help distinguish samples with different disease statuses (Fig. 2).

3.2 Enrichment analysis

Multiple GO functional terms were enriched for upregulated and downregulated genes. For upregulated genes, positive regulation of proteins targeting mitochondria, the glutathione derivative biosynthetic process, and mitochondrial translational termination were the primary functional terms that were enriched (Fig. 3). In contrast, cellular response to mechanical stimulus, centrosome localization, and thymus development were potential functions of downregulated genes (top 20 listed, Fig. 4). Meanwhile, the upregulated genes were implicated in 3 pathways (such as the intestinal immune network for immunoglobulin A (IgA) production, $P = 2.10 \times 10^{-2}$), whereas the downregulated genes were implicated in 15 pathways (such as endocytosis, $P = 4.61 \times 10^{-4}$; mitogen-activated protein kinase [MAPK] signaling pathway, $P = 1.22 \times 10^{-2}$) (Table 1). In particular, the downregulated transforming growth factor-beta receptor 2 (*TGFBR2*) and epidermal growth factor (*EGF*) were enriched in the MAPK signaling pathway.

3.3 PPI network analysis

The PPI network is shown in Fig. 5, presenting 212 nodes and 332 edges. In the PPI network, histone cluster 1, H2bj (*HIST1H2BJ*, down, degree = 18), histone cluster 1, H2ac (*HIST1H2AC*, down, degree = 17), *EGF* (down, degree = 16), and E1A binding protein p300 (*EP300*, down, degree = 15) were nodes with degrees higher than 10 and were thus con-

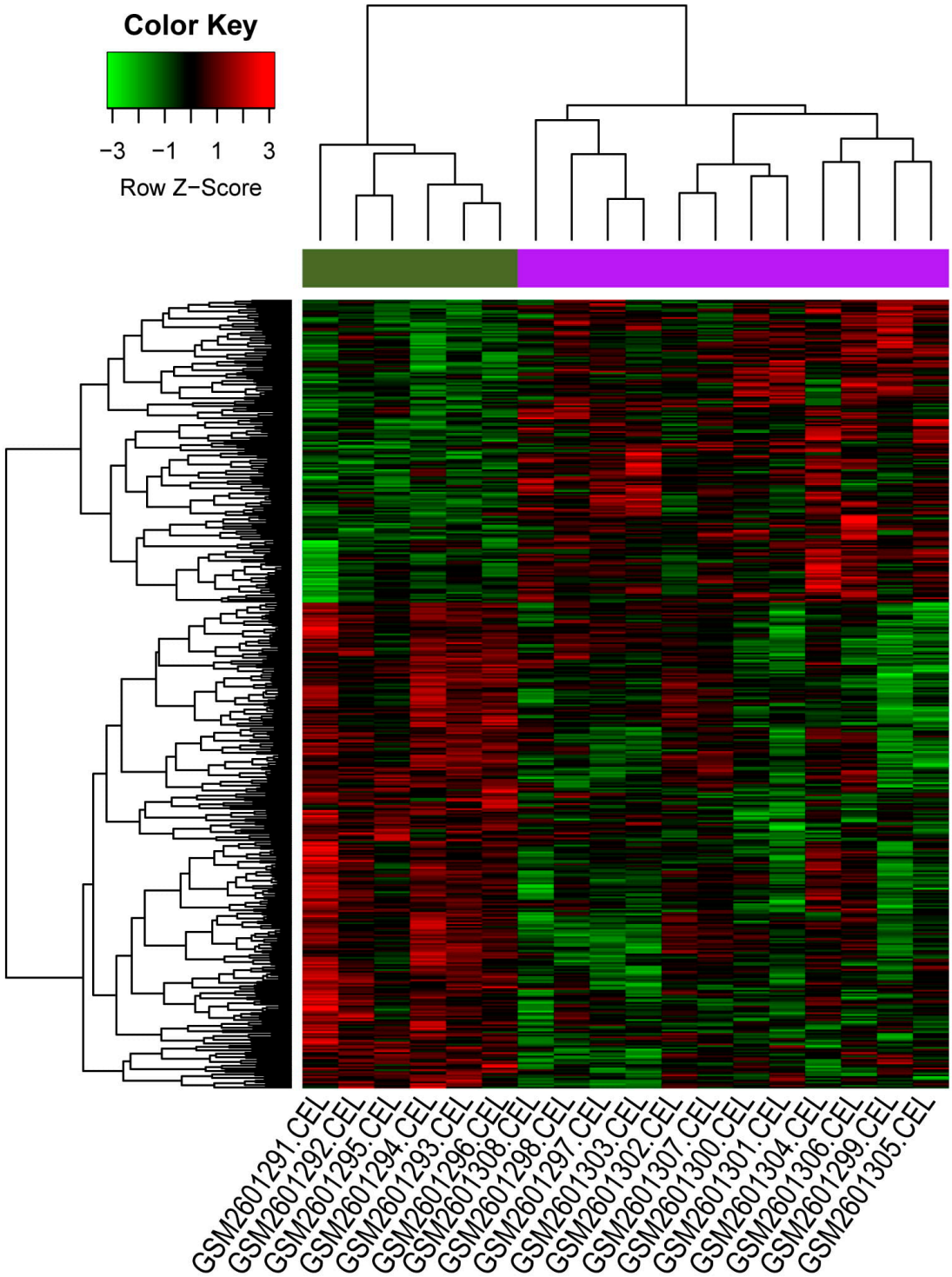

Fig. 2. The clustering heatmap of the differentially expressed genes (DEGs). Y-axis represents all DEGs, and X-axis represents all samples; the green and purple blocks in upper represent control group and CAD group, respectively.

sidered hub nodes. Moreover, four network modules were screened, including module A (score = 7; with seven nodes and 21 edges), module B (score = 6; with six nodes and 15 edges), module C (score = 6; with 6 nodes and 15 edges), and module D (score = 5.6; with 6 nodes and 14 edges) (Fig. 6). The results of the GO functional enrichment analysis of module nodes are listed in Table 2. The nodes in modules A, B, C, and D were mainly enriched in the inflammatory response ($P = 3.70 \times 10^{-6}$), protein ubiquitination involved in ubiquitin-dependent protein catabolic process ($P = 2.95 \times 10^{-6}$), protein transport ($P = 5.27 \times 10^{-3}$), and mitochondrial translational elongation ($P = 3.05 \times 10^{-9}$), respectively.

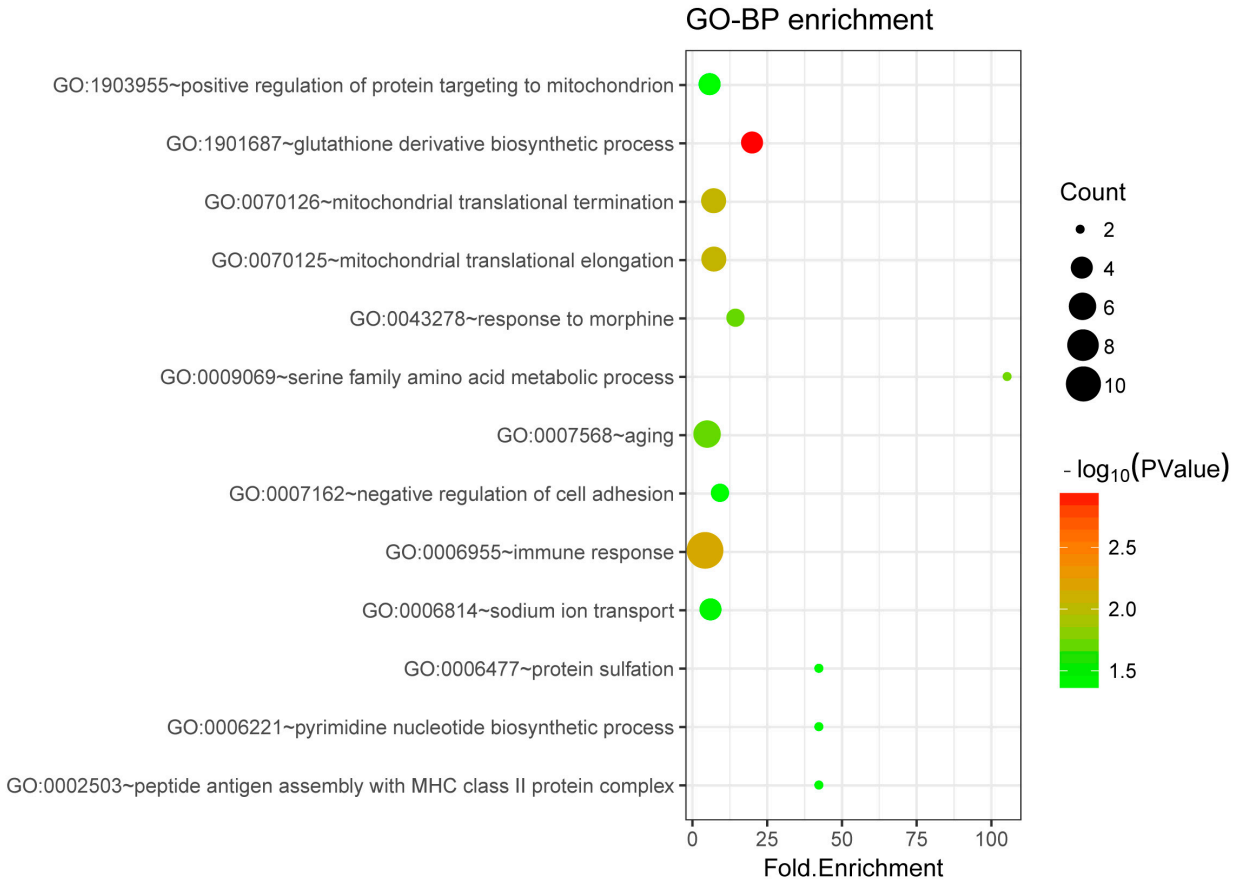

Fig. 3. The Gene Ontology (GO) terms enriched for upregulated genes. The size of a circle indicates the number of genes involved in the respective term. The color change from green to red suggests that the $-\log_{10}(P\text{-value})$ changes from small to large.

Table 1. Pathways enriched separately for the up- and down-regulated genes.

Category	Pathway ID	Pathway name	Count	*P* value	Genes
UP	hsa04672	Intestinal immune network for IgA production	4	2.10×10^{-2}	*CD86, IL15, HLA-DMB, HLA-DMA*
	hsa05150	*Staphylococcus aureus* infection	4	3.02×10^{-2}	*C3AR1, C3, HLA-DMB, HLA-DMA*
	hsa00561	Glycerolipid metabolism	4	3.62×10^{-2}	*AKR1A1, DGKH, AGK, ALDH3A2*
DOWN	hsa04144	Endocytosis	14	4.61×10^{-4}	*CHMP2A, RAB5B, TGFBR2, CXCR1, CXCR2, VPS37C, EPS15L1, KIT, IGF2R, HSPA6, GIT2, RAB11A, EGF, IQSEC1*
	hsa05220	Chronic myeloid leukemia	7	1.42×10^{-3}	*E2F3, GAB2, SOS1, STAT5B, TGFBR2, SOS2, RAF1*
	hsa04068	FoxO signaling pathway	9	2.09×10^{-3}	*EP300, S1PR4, SOS1, PRKAB2, TGFBR2, SOS2, RAF1, EGF, BCL2L11*
	hsa05219	Bladder cancer	5	5.18×10^{-3}	*RPS6KA5, E2F3, RAF1, DAPK2, EGF*
	hsa04010	MAPK signaling pathway	11	1.22×10^{-2}	*RPS6KA5, SOS1, TGFBR2, SOS2, MAP2K4, HSPA6, RAF1, CACNB4, RAPGEF2, EGF, DUSP6*
	hsa05223	Non-small cell lung cancer	5	1.54×10^{-2}	*E2F3, SOS1, SOS2, RAF1, EGF*
	hsa05221	Acute myeloid leukemia	5	1.54×10^{-2}	*SOS1, STAT5B, SOS2, RAF1, KIT*
	hsa04012	ErbB signaling pathway	6	1.68×10^{-2}	*SOS1, STAT5B, SOS2, MAP2K4, RAF1, EGF*
	hsa05215	Prostate cancer	6	1.75×10^{-2}	*E2F3, EP300, SOS1, SOS2, RAF1, EGF*
	hsa05212	Pancreatic cancer	5	2.53×10^{-2}	*E2F3, RALBP1, TGFBR2, RAF1, EGF*
	hsa05214	Glioma	5	2.53×10^{-2}	*E2F3, SOS1, SOS2, RAF1, EGF*
	hsa04664	Fc epsilon RI signaling pathway	5	2.93×10^{-2}	*GAB2, SOS1, SOS2, MAP2K4, RAF1*
	hsa05200	Pathways in cancer	13	3.74×10^{-2}	*E2F3, RALBP1, TGFBR2, STAT5B, RAF1, FADD, KIT, DAPK2, EP300, SOS1, SOS2, TPR, EGF*
	hsa05161	Hepatitis B	7	3.87×10^{-2}	*E2F3, EP300, DDX3X, STAT5B, MAP2K4, RAF1, FADD*
	hsa00531	Glycosaminoglycan degradation	3	4.16×10^{-2}	*HYAL2, IDS, GALNS*

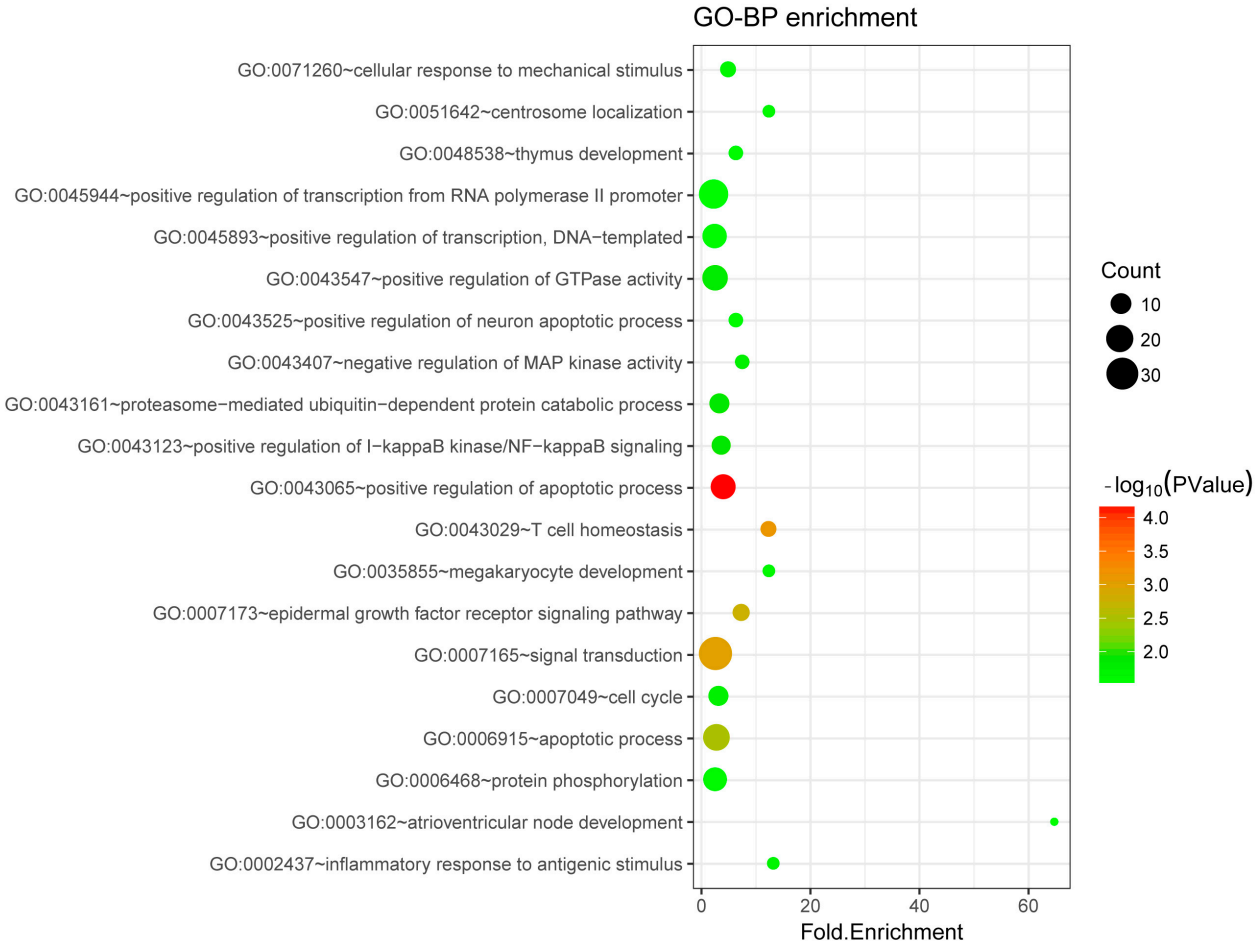

Fig. 4. The Gene Ontology (GO) terms enriched for downregulated genes. The size of a circle indicates the number of genes involved in the respective term. The color change from green to red suggests that the $-\log_{10}$(*P*-value) changes from small to large.

3.4 TF-miRNA target regulatory network analysis

Following the prediction of 2 TFs (*E2F1* and *FOXK1*) and 5 miRNAs (*miR-122A*, *miR-516-5P*, *miR-507*, *miR-342*, and *miR-520F*), 172 regulatory pairs were obtained (involving 29 upregulated and 83 downregulated genes). Subsequently, we built a TF-miRNA target regulatory network (Fig. 7). In the regulatory network, *miR-122A* can target both low-density lipoprotein (LDL) receptor-related protein 10 (*LRP10*) and IQ motif-containing GTPase-activating protein 1 (*IQGAP1*).

3.5 Validation with CTD database

In the CTD database, a total of 25,384 genes and 149 pathways were found to be associated with CAD. The Venn analysis identified 429 overlapping genes between CAD-associated genes and 456 DEGs, including *TGFBR2*, *EGF*, *LRP10*, and *IQGAP1* (Fig. 8A and **Supplemental Table 1**). Similarly, we screened 10 overlapping pathways between CAD-associated pathways and 18 significant KEGG pathways, including the MAPK signaling pathway (Fig. 8B and Table 3). These results suggest that identified genes and pathways are important in CAD and could be implicated in CAD pathogenesis.

4. Discussion

In the present study, we identified 456 DEGs (including 175 upregulated and 281 downregulated genes) between CAD and control samples. In the PPI network, *EGF* (down, degree = 16) was a hub node. Additionally, we screened four significant network modules (modules A, B, C, and D) and observed that each node was individually implicated in the inflammatory response, protein ubiquitination involved in ubiquitin-dependent protein catabolic process, protein transport, and mitochondrial translational elongation. Furthermore, we built a TF-miRNA target regulatory network.

In patients with CAD, *TGFBR2* polymorphism is correlated with the risk of sudden cardiac arrest induced by ventricular arrhythmias, suggesting that genetic variations in the TGF signaling pathway could influence susceptibility to sudden cardiac arrest [37]. *TGFBR1* is reportedly overexpressed in patients with left ventricular dysfunction and is thus considered a potential prognostic factor after acute myocardial infarction [38]. The mRNA expression levels of *EGFR* in atheromatous lesions could be a promising prognostic biomarker for predicting the stimulatory growth factor-induced increase in smooth muscle cell proliferation [39].

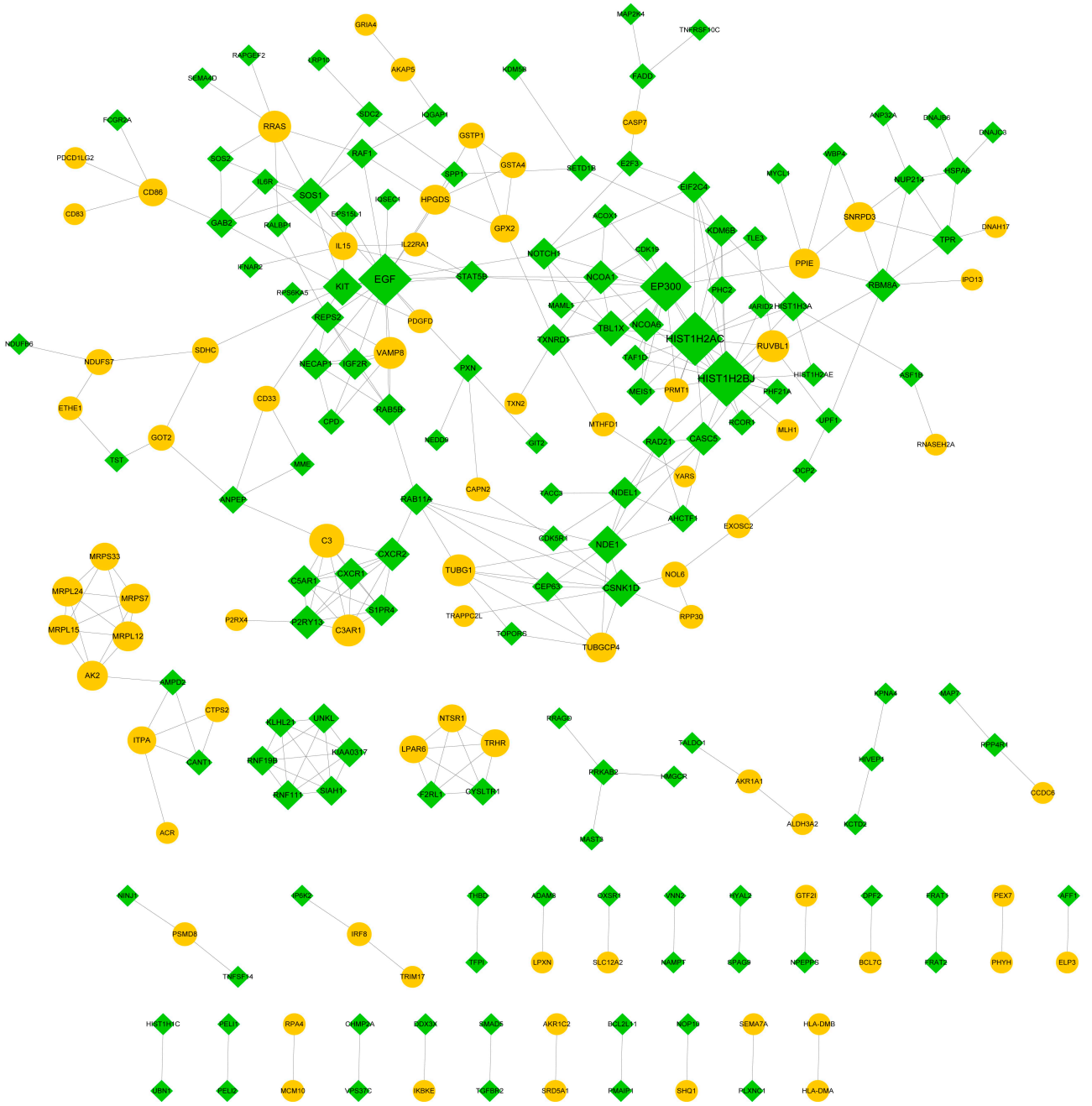

Fig. 5. The protein-protein interaction (PPI) network. Yellow circles and green prisms indicate upregulated and downregulated genes, respectively. The nodes with higher degrees are large.

Circulating *miR-23a* could serve as a diagnostic biomarker to indicate the presence and severity of coronary lesions in patients with CAD. Moreover, *miR-23a* regulates vasculogenesis in CAD by inhibiting *EGFR* expression [40]. In the present study, both *TGFBR2* and *EGF* were involved in the MAPK signaling pathway, thus indicating their potential roles in CAD development.

Plasma levels of *miR-122* and *miR-370*, which are upregulated in patients with hyperlipidemia, are positively associated with CAD severity; therefore, they may be correlated with the development and progression of CAD in patients with hyperlipidemia [41]. The expression of circulating *miR-122-5p* is reportedly elevated in patients with acute myocardial infarction, suggesting its application as a promising biomarker [42, 43]. The plasma levels of *miR-122*, *miR-140-3p*, *miR-720*, *miR-2861*, and *miR-3149* are higher in acute coronary syndrome samples than in control samples; thus, they can be employed as potential markers in patients with acute coronary syndrome [44]. These results indicate that *miR-122* plays a critical role in CAD pathogenesis.

LRP is known to possess biological functions in multiple vascular biology-associated processes. Moreover, *LRP* poly-

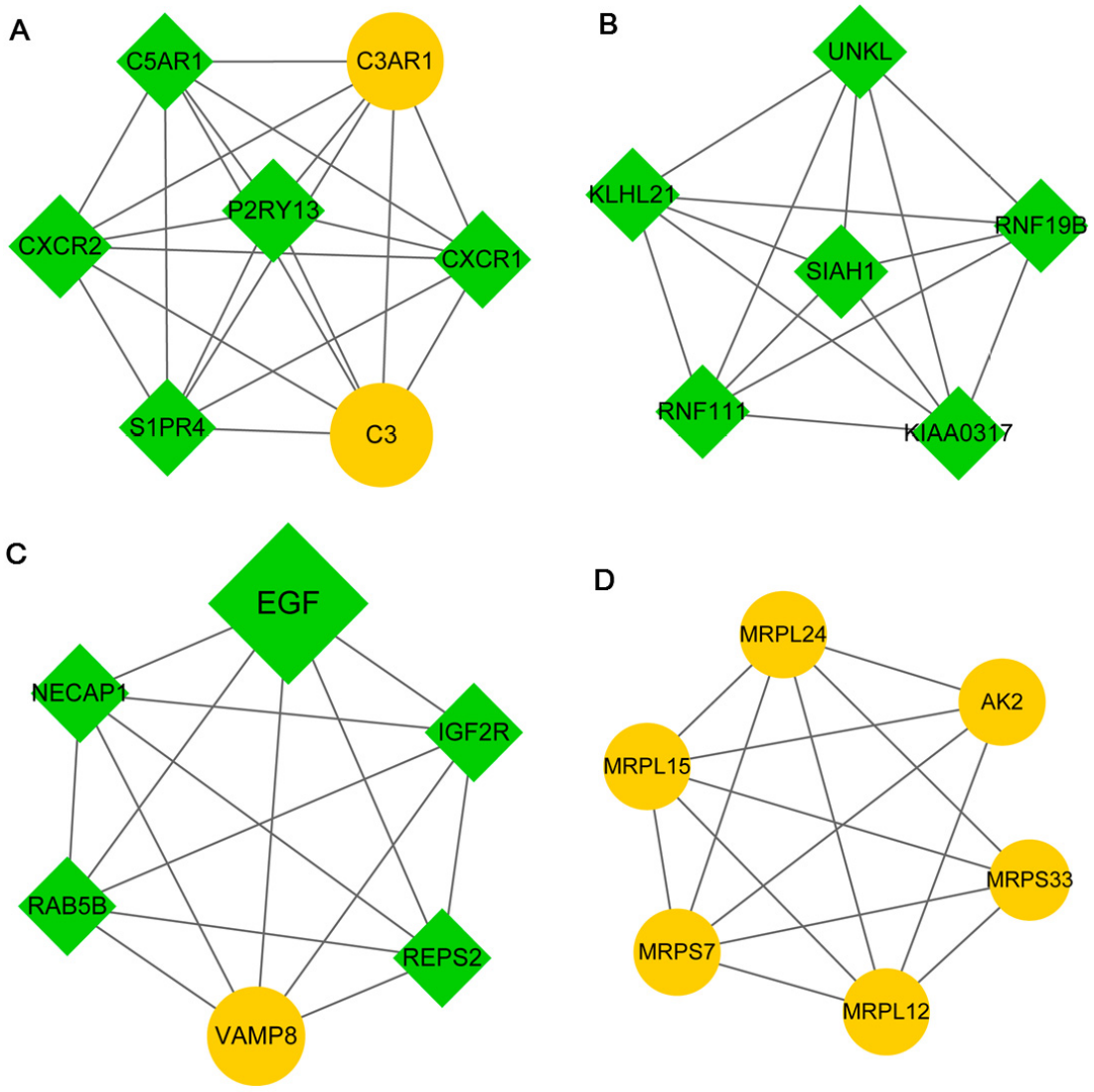

Fig. 6. Modules A (A), B (B), C (C), and D (D) identified from the protein-protein interaction (PPI) network. Yellow circles and green prisms indicate upregulated and downregulated genes, respectively. The nodes with higher degrees are large.

morphisms are risk factors, especially in Caucasians with premature CAD [45]. In cardiac fibroblasts, *LRP1* contributes to the expression of matrix metallopeptidase 9 (*MMP9*), which has been associated with ventricular remodeling following myocardial infarction [46]. *IQGAP1* reportedly affects neovascularization after ischemia by mediating endothelial cell-regulated angiogenesis, macrophage infiltration, and reactive oxygen species production; therefore, *IQGAP1* is a valuable therapeutic target for ischemic cardiovascular diseases [47, 48]. As a scaffold for the extracellular signal-regulated kinase (ERK)1/2 cascade, *IQGAP1* mediates the integration of hypertrophy and survival signals in the heart, facilitating left ventricular remodeling following pressure overload [49]. Therefore, both *LRP10* and *IQGAP1* were targeted by *miR-122A* in the regulatory network, implying a probable correlation between *miR-122A* and CAD via the regulation of *LRP10* and *IQGAP1*.

5. Conclusions

In total, 456 DEGs were screened in CAD samples. Herein, we revealed the probable involvement of *TGFBR2*, *EGF*, *LRP10*, *IQGAP1*, and *miR-122* in CAD pathogenesis. The functions of these genes and miRNAs in CAD pathogenesis need to be comprehensively validated in future experimental research.

Author contributions

Conception and design of the research: WZ and XL; acquisition of data: NW, TL and GZ; analysis and interpretation of data: SF and LL; Statistical analysis: XL and YH; drafting the manuscript: YD; revision of manuscript for important intellectual content: WZ. All authors read and approved the final manuscript.

Table 2. The GO functional terms enriched for the nodes in modules A, B, C, and D.

Module	Biological process	Count	*P* value	Genes
Module A	GO:0006954 inflammatory response	5	$3.70E \times 10^{-6}$	*C3AR1, C5AR1, C3, CXCR1, CXCR2*
	GO:0045766 positive regulation of angiogenesis	4	6.17×10^{-6}	*C3AR1, C5AR1, C3, CXCR2*
	GO:0006935 chemotaxis	4	7.37×10^{-6}	*C3AR1, C5AR1, CXCR1, CXCR2*
	GO:0007204 positive regulation of cytosolic calcium ion concentration	4	9.77×10^{-6}	*C3AR1, C5AR1, S1PR4, CXCR2*
	GO:0090023 positive regulation of neutrophil chemotaxis	3	2.45×10^{-6}	*C3AR1, C5AR1, CXCR2*
	GO:0010575 positive regulation of vascular endothelial growth factor production	3	3.72×10^{-5}	*C3AR1, C5AR1, C3*
	GO:0030449 regulation of complement activation	3	4.61×10^{-5}	*C3AR1, C5AR1, C3*
	GO:0007200 phospholipase C-activating G-protein coupled receptor signaling pathway	3	2.26×10^{-4}	*C3AR1, C5AR1, CXCR2*
	GO:0038112 interleukin-8-mediated signaling pathway	2	7.15×10^{-4}	*CXCR1, CXCR2*
	GO:0007186 G-protein coupled receptor signaling pathway	4	2.71×10^{-3}	*C3AR1, C3, S1PR4, CXCR1*
	GO:0010759 positive regulation of macrophage chemotaxis	2	3.92×10^{-3}	*C3AR1, C5AR1*
	GO:0002407 dendritic cell chemotaxis	2	6.06×10^{-3}	*CXCR1, CXCR2*
	GO:0006955 immune response	3	8.80×10^{-3}	*C5AR1, C3, S1PR4*
	GO:0007202 activation of phospholipase C activity	2	9.26×10^{-3}	*C5AR1, S1PR4*
	GO:0031623 receptor internalization	2	1.53×10^{-2}	*CXCR1, CXCR2*
	GO:0006968 cellular defense response	2	2.20×10^{-2}	*C5AR1, CXCR2*
	GO:0060326 cell chemotaxis	2	2.30×10^{-2}	*C3AR1, C5AR1*
	GO:0030593 neutrophil chemotaxis	2	2.34×10^{-2}	*C5AR1, CXCR2*
	GO:0070098 chemokine-mediated signaling pathway	2	2.51×10^{-2}	*CXCR1, CXCR2*
	GO:0050900 leukocyte migration	2	4.28×10^{-2}	*C3AR1, C5AR1*
Module B	GO:0042787 protein ubiquitination involved in ubiquitin-dependent protein catabolic process	4	2.95×10^{-6}	*KLHL21, SIAH1, RNF19B, RNF111*
	GO:0000209 protein polyubiquitination	4	5.14×10^{-6}	*SIAH1, RNF19B, UNKL, RNF111*
	GO:0043161 proteasome-mediated ubiquitin-dependent protein catabolic process	2	4.75×10^{-2}	*SIAH1, RNF111*
Module C	GO:0015031 protein transport	3	5.27×10^{-3}	*RAB5B, VAMP8, NECAP1*
	GO:0007173 epidermal growth factor receptor signaling pathway	2	1.66×10^{-2}	*REPS2, EGF*
Module D	GO:0070125 mitochondrial translational elongation	5	3.05×10^{-9}	*MRPL24, MRPL12, MRPS33, MRPL15, MRPS7*
	GO:0070126 mitochondrial translational termination	5	3.19×10^{-9}	*MRPL24, MRPL12, MRPS33, MRPL15, MRPS7*
	GO:0006412 translation	4	3.31×10^{-5}	*MRPL24, MRPS33, MRPL15, MRPS7*

Table 3. The 10 overlapped pathways in VENN analysis for pathways.

Disease name	Disease ID	Category	Term	Count	*P* value	Genes
CAD	MESH:D003324	KEGG_PATHWAY	hsa04672:Intestinal immune network for IgA production	4	2.10×10^{-2}	*CD86, IL15, HLA-DMB, HLA-DMA*
CAD	MESH:D003324	KEGG_PATHWAY	hsa00561:Glycerolipid metabolism	4	3.62×10^{-2}	*AKR1A1, DGKH, AGK, ALDH3A2*
CAD	MESH:D003325	KEGG_PATHWAY	hsa04144:Endocytosis	14	4.61×10^{-4}	*CHMP2A, RAB5B, TGFBR2, CXCR1, CXCR2, VPS37C, EPS15L1, KIT, IGF2R, HSPA6, GIT2, RAB11A, EGF, IQSEC1*
CAD	MESH:D003326	KEGG_PATHWAY	hsa04068:FoxO signaling pathway	9	2.09×10^{-3}	*EP300, S1PR4, SOS1, PRKAB2, TGFBR2, SOS2, RAF1, EGF, BCL2L11*
CAD	MESH:D003327	KEGG_PATHWAY	hsa05219:Bladder cancer	5	5.18×10^{-3}	*RPS6KA5, E2F3, RAF1, DAPK2, EGF*
CAD	MESH:D003328	KEGG_PATHWAY	hsa04010:MAPK signaling pathway	11	1.22×10^{-2}	*RPS6KA5, SOS1, TGFBR2, SOS2, MAP2K4, HSPA6, RAF1, CACNB4, RAPGEF2, EGF, DUSP6*
CAD	MESH:D003329	KEGG_PATHWAY	hsa05215:Prostate cancer	6	1.75×10^{-2}	*E2F3, EP300, SOS1, SOS2, RAF1, EGF*
CAD	MESH:D003330	KEGG_PATHWAY	hsa05212:Pancreatic cancer	5	2.53×10^{-2}	*E2F3, RALBP1, TGFBR2, RAF1, EGF*
CAD	MESH:D003331	KEGG_PATHWAY	hsa05200:Pathways in cancer	13	3.74×10^{-2}	*E2F3, RALBP1, TGFBR2, STAT5B, RAF1, FADD, KIT, DAPK2, EP300, SOS1, SOS2, TPR, EGF*
CAD	MESH:D003332	KEGG_PATHWAY	hsa05161:Hepatitis B	7	3.87×10^{-2}	*E2F3, EP300, DDX3X, STAT5B, MAP2K4, RAF1, FADD*

CAD, coronary artery disease.

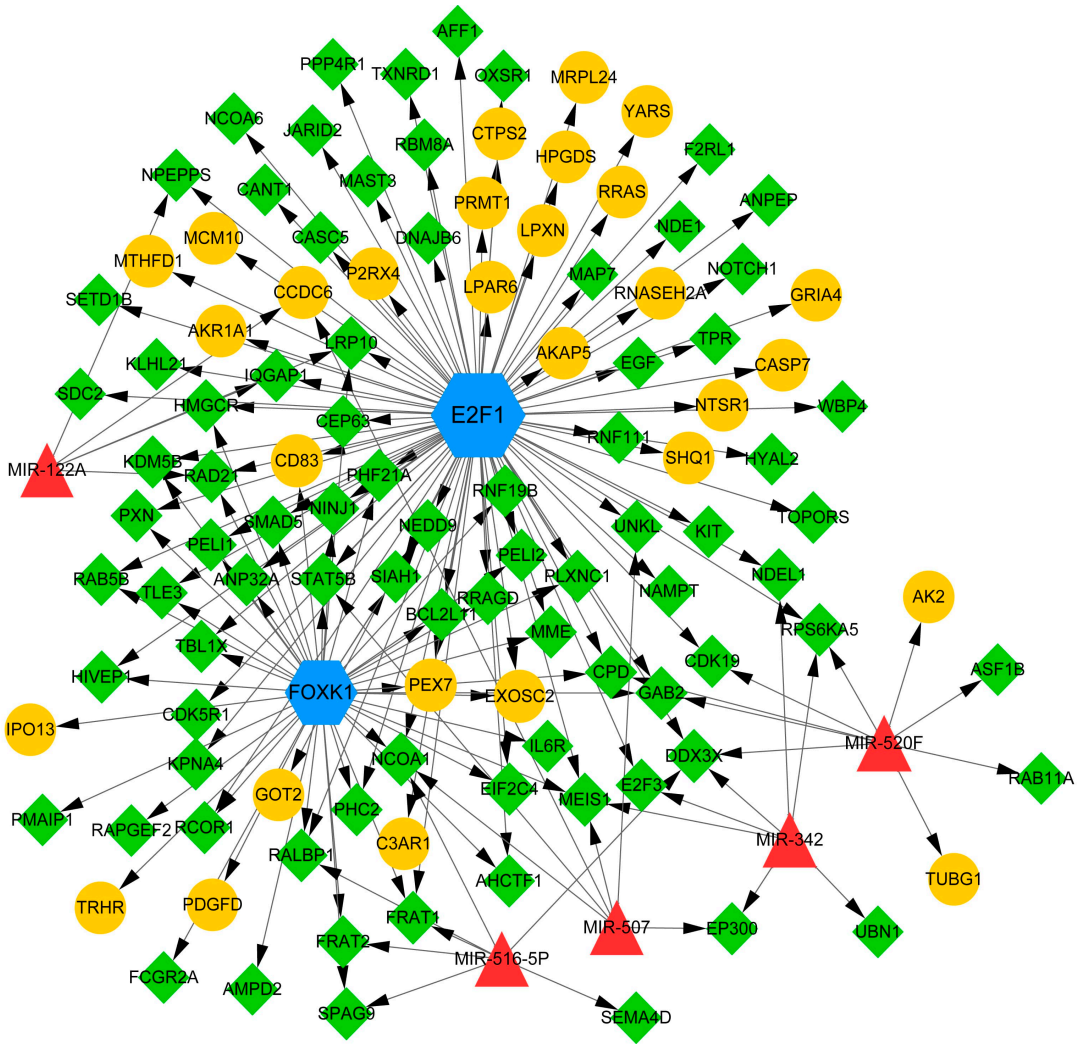

Fig. 7. The transcription factor (TF)-microRNA (miRNA) target regulatory network. Yellow circles and green prisms indicate upregulated and downregulated genes, respectively. Blue hexagons and red triangles indicate TFs and miRNAs, respectively. Arrows indicate regulatory directions.

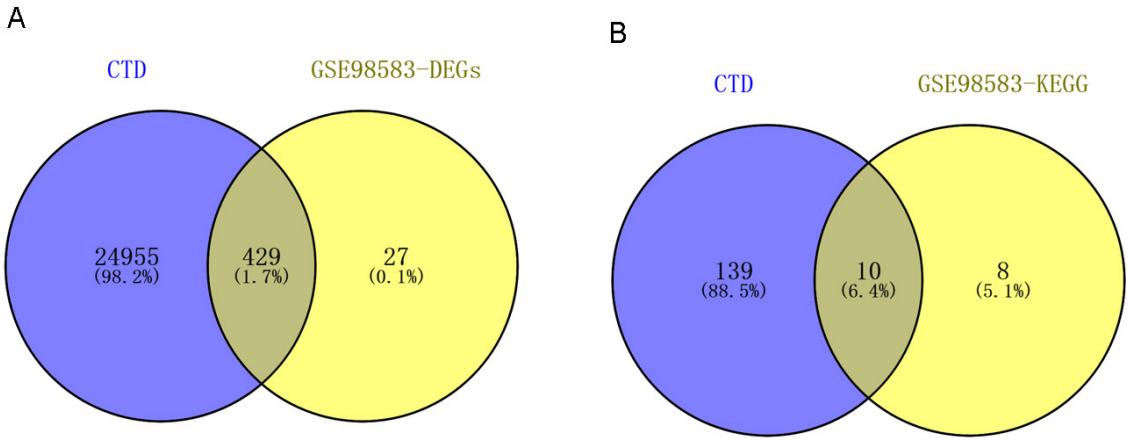

Fig. 8. The results of Venn analysis using the CTD database. (A) Venn diagram showing 429 overlapping genes between CAD-associated genes and differentially expressed genes. (B) Venn diagram showing 10 overlapping pathways between CAD-associated pathways and 18 significant KEGG pathways. CTD, Comparative Toxicogenomics Database; CAD, Coronary artery disease; KEGG, Kyoto Encyclopedia of Genes and Genomes.

Ethics approval and consent to participate

Not applicable.

Acknowledgment

Thanks to all the peer reviewers and academic editors for their opinions and suggestions.

Funding

This work was supported by the National Natural Science Foundation of China (No. 81600207), Excellent Youth Fund of Jilin Provincial Science and Technology Department (No. 20190103090JH), "13th five year plan" science and technology research project of Jilin Provincial Department of Education (No. JJKH20200898KJ), Science and Technology Department of Jilin Province (No. 20190304054YY), "Xinglin scholar project" of Changchun University of traditional Chinese Medicine (No. 2019RS01) and College Project Grant (No. 2018KJ01).

Conflict of interest

The authors declare no conflict of interest.

Supplementary material

Supplementary material associated with this article can be found, in the online version, at https://rcm.imrpress.com/EN/10.31083/j.rcm2203103.

Data availability

The data used to support the findings of this study are available from the corresponding author upon request.

References

[1] Malakar AK, Choudhury D, Halder B, Paul P, Uddin A, Chakraborty S. A review on coronary artery disease, its risk factors, and therapeutics. Journal of Cellular Physiology. 2019; 234: 16812–16823.

[2] Fox KAA, Metra M, Morais J, Atar D. The myth of 'stable' coronary artery disease. Nature Reviews Cardiology. 2020; 17: 9–21.

[3] Mehta PK, Wei J, Wenger NK. Ischemic heart disease in women: a focus on risk factors. Trends in Cardiovascular Medicine. 2015; 25: 140–151.

[4] Khera AV, Kathiresan S. Genetics of coronary artery disease: discovery, biology and clinical translation. Nature Reviews Genetics. 2017; 18: 331–344.

[5] Arsenault BJ, Després J. Cardiovascular disease prevention: lifestyle attenuation of genetic risk. Nature Reviews Cardiology. 2017; 14: 187–188.

[6] Faroux L, Guimaraes L, Wintzer-Wehekind J, Junquera L, Ferreira-Neto AN, Del Val D, *et al.* Coronary Artery Disease and Transcatheter Aortic Valve Replacement: JACC State-of-the-Art Review. Journal of the American College of Cardiology. 2019; 74: 362–372.

[7] GBD 2015 Mortality and Causes of Death Collaborators. Global, regional, and national life expectancy, all-cause mortality, and cause-specific mortality for 249 causes of death, 1980–2015: a systematic analysis for the Global Burden of Disease Study 2015. Lancet. 2016; 388: 1459–1544.

[8] Wang L, Hauser ER, Shah SH, Pericak-Vance MA, Haynes C, Crosslin D, *et al.* Peakwide mapping on chromosome 3q13 identifies the kalirin gene as a novel candidate gene for coronary artery disease. American Journal of Human Genetics. 2007; 80: 650–663.

[9] Eiras S, Teijeira-Fernández E, Shamagian LG, Fernandez AL, Vazquez-Boquete A, Gonzalez-Juanatey JR. Extension of coronary artery disease is associated with increased IL-6 and decreased adiponectin gene expression in epicardial adipose tissue. Cytokine. 2008; 43: 174–180.

[10] Lim GB. Coronary artery disease: IL-6 signaling linked with CHD. Nature Reviews Cardiology. 2012; 9: 313.

[11] Tian Q, Liu M, Tang C, Xue L, Pang Y, Qi Y. Association of Circulating Neuregulin-4 with Presence and Severity of Coronary Artery Disease. International Heart Journal. 2019; 60: 45–49.

[12] Chen H, Mo N, Zhang Y, Su G, Wu H, Pei F. Role of Gene Polymorphisms/Haplotypes and Plasma Level of TGF-β1 in Susceptibility to in-Stent Restenosis Following Coronary Implantation of Bare Metal Stent in Chinese Han Patients. International Heart Journal. 2018; 59: 161–169.

[13] Jin Y, Yang C, Xu X, Cao J, Feng Q, Yang J. MiR-214 regulates the pathogenesis of patients with coronary artery disease by targeting VEGF. Molecular and Cellular Biochemistry. 2015; 402: 111–122.

[14] Tabuchi T, Satoh M, Itoh T, Nakamura M. MicroRNA-34a regulates the longevity-associated protein SIRT1 in coronary artery disease: effect of statins on SIRT1 and microRNA-34a expression. Clinical Science. 2012; 123: 161–171.

[15] Han H, Qu G, Han C, Wang Y, Sun T, Li F, *et al.* MiR-34a, miR-21 and miR-23a as potential biomarkers for coronary artery disease: a pilot microarray study and confirmation in a 32 patient cohort. Experimental & Molecular Medicine. 2015; 47: e138.

[16] Schulte C, Molz S, Appelbaum S, Karakas M, Ojeda F, Lau DM, *et al.* miRNA-197 and miRNA-223 Predict Cardiovascular Death in a Cohort of Patients with Symptomatic Coronary Artery Disease. PLos ONE. 2015; 10: e0145930.

[17] Bai Y, Zhang Q, Su Y, Pu Z, Li K. Modulation of the Proliferation/Apoptosis Balance of Vascular Smooth Muscle Cells in Atherosclerosis by lncRNA-MEG3 via Regulation of miR-26a/Smad1 Axis. International Heart Journal. 2019; 60: 444–450.

[18] Borovecki F, Lovrecic L, Zhou J, Jeong H, Then F, Rosas HD, *et al.* Genome-wide expression profiling of human blood reveals biomarkers for Huntington's disease. Proceedings of the National Academy of Sciences. 2005; 102: 11023–11028.

[19] Osman I, Bajorin DF, Sun T, Zhong H, Douglas D, Scattergood J, *et al.* Novel Blood Biomarkers of Human Urinary Bladder Cancer. Clinical Cancer Research. 2006; 12: 3374–3380.

[20] Wingrove JA, Daniels SE, Sehnert AJ, Tingley W, Elashoff MR, Rosenberg S, *et al.* Correlation of peripheral-blood gene expression with the extent of coronary artery stenosis. Circulation: Cardiovascular Genetics. 2008; 1: 31–38.

[21] Sinnaeve PR, Donahue MP, Grass P, Seo D, Vonderscher J, Chibout SD, *et al.* Gene expression patterns in peripheral blood correlate with the extent of coronary artery disease. PLoS ONE. 2009; 4: e7037.

[22] Taurino C, Miller WH, McBride MW, McClure JD, Khanin R, Moreno MU, *et al.* Gene expression profiling in whole blood of patients with coronary artery disease. Clinical Science. 2010; 119: 335–343.

[23] Kashyap S, Kumar S, Agarwal V, Misra DP, Phadke SR, Kapoor A. Gene expression profiling of coronary artery disease and its relation with different severities. J Genet. 2018;97: 853–867.

[24] Carvalho BS, Irizarry RA. A framework for oligonucleotide microarray preprocessing. Bioinformatics. 2010; 26: 2363–2367.

[25] Smyth GK. limma: Linear Models for Microarray Data. Springer: New York, NY, USA. 2005.

[26] Huang DW, Sherman BT, Lempicki RA. Systematic and integrative analysis of large gene lists using DAVID bioinformatics resources. Nature Protocols. 2008; 4: 44–57.

[27] Blake JA, Christie KR, Dolan ME, Drabkin HJ, Hill DP, Ni L, *et al.* Gene Ontology Consortium: going forward. Nucleic Acids Research. 2015; 43: D1049–D1056.

[28] Kanehisa M, Sato Y, Kawashima M, Furumichi M, Tanabe M. KEGG as a reference resource for gene and protein annotation. Nucleic Acids Research. 2016; 44: D457–D462.

[29] Franceschini A, Szklarczyk D, Frankild S, Kuhn M, Simonovic M, Roth A, *et al.* STRING v9.1: protein-protein interaction networks, with increased coverage and integration. Nucleic Acids Research. 2013; 41: D808–D815.
[30] Smoot ME, Ono K, Ruscheinski J, Wang P, Ideker T. Cytoscape 2.8: new features for data integration and network visualization. Bioinformatics. 2011; 27: 431–432.
[31] Tang Y, Li M, Wang J, Pan Y, Wu F. CytoNCA: a cytoscape plugin for centrality analysis and evaluation of protein interaction networks. BioSystems. 2015; 127: 67–72.
[32] Bader GD, Hogue CWV. An automated method for finding molecular complexes in large protein interaction networks. BMC Bioinformatics. 2003; 4: 2.
[33] Janky R, Verfaillie A, Imrichová H, Van de Sande B, Standaert L, Christiaens V, *et al.* IRegulon: from a gene list to a gene regulatory network using large motif and track collections. PLoS Computational Biology. 2014; 10: e1003731.
[34] Wang J, Duncan D, Shi Z, Zhang B. WEB-based GEne SeT AnaLysis Toolkit (WebGestalt): update 2013. Nucleic Acids Research. 2013; 41: W77–W83.
[35] Davis AP, Murphy CG, Rosenstein MC, Wiegers TC, Mattingly CJ. The Comparative Toxicogenomics Database facilitates identification and understanding of chemical-gene-disease associations: arsenic as a case study. BMC Medical Genomics. 2008; 1: 48.
[36] Mattingly CJ, Rosenstein MC, Colby GT, Forrest Jr JN, Boyer JL. The Comparative Toxicogenomics Database (CTD): a resource for comparative toxicological studies. Journal of Experimental Zoology. 2006; 305: 689–692.
[37] Tseng ZH, Vittinghoff E, Musone SL, Lin F, Whiteman D, Pawlikowska L, *et al.* Association of TGFBR2 polymorphism with risk of sudden cardiac arrest in patients with coronary artery disease. Heart Rhythm. 2009; 6: 1745–1750.
[38] Devaux Y, Bousquenaud M, Rodius S, Marie P, Maskali F, Zhang L, *et al.* Transforming growth factor β receptor 1 is a new candidate prognostic biomarker after acute myocardial infarction. BMC Medical Genomics. 2011; 4: 83.
[39] Bauriedel G, Heidemann P, Klingel K, Windstetter U, Höfling B, Kandolf R. *In situ* detection of EGF receptor mRNA in arteriosclerotic lesions in man: implications for the proliferative activity of smooth muscle cells. Zeitschrift Für Kardiologie. 1992; 81: 519–524. (In German)
[40] Wang S, He W, Wang C. MiR-23a Regulates the Vasculogenesis of Coronary Artery Disease by Targeting Epidermal Growth Factor Receptor. Cardiovascular Therapeutics. 2016; 34: 199–208.
[41] Gao W, He H, Wang Z, Zhao H, Lian X, Wang Y, *et al.* Plasma levels of lipometabolism-related miR-122 and miR-370 are increased in patients with hyperlipidemia and associated with coronary artery disease. Lipids in Health and Disease. 2012; 11: 55.
[42] Yao X, Lu X, Yan C, Wan Q, Cheng G, Li Y. Circulating miR-122-5p as a potential novel biomarker for diagnosis of acute myocardial infarction. International Journal of Clinical and Experimental Pathology. 2015; 8: 16014–16019.
[43] Cortez-Dias N, Costa MC, Carrilho-Ferreira P, Silva D, Jorge C, Calisto C, *et al.* Circulating miR-122-5p/miR-133b Ratio is a Specific Early Prognostic Biomarker in Acute Myocardial Infarction. Circulation Journal. 2016; 80: 2183–2191.
[44] Li X, Yang Y, Wang L, Qiao S, Lu X, Wu Y, *et al.* Plasma miR-122 and miR-3149 Potentially Novel Biomarkers for Acute Coronary Syndrome. PLoS ONE. 2015; 10: e0125430.
[45] Pocathikorn A, Granath B, Thiry E, Van Leuven F, Taylor R, Mamotte C. Influence of exonic polymorphisms in the gene for LDL receptor-related protein (LRP) on risk of coronary artery disease. Atherosclerosis. 2003; 168: 115–121.
[46] Revuelta-López E, Soler-Botija C, Nasarre L, Benitez-Amaro A, de Gonzalo-Calvo D, Bayes-Genis A, *et al.* Relationship among LRP1 expression, Pyk2 phosphorylation and MMP-9 activation in left ventricular remodelling after myocardial infarction. Journal of Cellular and Molecular Medicine. 2017; 21: 1915–1928.
[47] Urao N, Razvi M, Oshikawa J, McKinney RD, Chavda R, Bahou WF, *et al.* IQGAP1 is involved in post-ischemic neovascularization by regulating angiogenesis and macrophage infiltration. PLoS ONE. 2010; 5: e13440.
[48] Yamaoka-Tojo M, Ushio-Fukai M, Hilenski L, Dikalov SI, Chen YE, Tojo T, *et al.* IQGAP1, a novel vascular endothelial growth factor receptor binding protein, is involved in reactive oxygen species—dependent endothelial migration and proliferation. Circulation Research. 2004; 95: 276–283.
[49] Sbroggiò M, Carnevale D, Bertero A, Cifelli G, De Blasio E, Mascio G, *et al.* IQGAP1 regulates ERK1/2 and AKT signalling in the heart and sustains functional remodelling upon pressure overload. Cardiovascular Research. 2011; 91: 456–464.